applied sciences

MDPI

Article

Sensitivity Analysis of Different Hydrothermal Characteristics in the Variable Thermodynamic Processes of Soft Clay Rock

Tao Wang [1,2,3,4,*], Huixi Lin [1,2], Kexiong Ren [3], Jian Gao [1,2] and Di Wang [4]

[1] SINOPEC Key Laboratory of Geology and Resources in Deep Stratum, Beijing 102206, China
[2] SINOPEC Petroleum Exploration and Production Research Institute, Beijing 102206, China
[3] The Natural Resources and Planning Bureau of Yiling District, Yichang 443100, China
[4] State Key Laboratory for Geomechanics and Deep Underground Engineering, School of Mechanics and Civil Engineering, China University of Mining and Technology, Xuzhou 221116, China
* Correspondence: taowang@cumt.edu.cn

Abstract: Artificial ground freezing technology is the most important construction method of complex water-bearing soft clay rock. The thermodynamic properties of soft clay rock are important evidence for the design and construction of space resources development, and the variable hydrothermal parameter can directly affect the uncertain thermodynamic properties of soft clay rock. In this work, an array of field experiments on the soft clay rock are carried out, and the anisotropic spatial variations of hydrothermal parameters of soft clay rock are obtained. The statistical variability characteristics of variable hydrothermal parameters are estimated. A stochastic coupling model of soft clay rock with heat conduction and porous flow is proposed, and the uncertain thermodynamic properties of soft clay rock are computed by the self-compiled program. Model validation with the experimental and numerical temperatures is also presented. According to the relationship between anisotropic spatial variations and statistical variability characteristics for the different random field correlation models, the effects of the autocorrelation function, coefficient of variation, and autocorrelation distance of variable hydrothermal parameters on the uncertain thermodynamic properties of soft clay rock are analyzed. The results show that the proposed stochastic analysis model for the thermal characteristics of soft clay rock, considering the spatial variability of frozen soil layers, is scientifically reasonable. The maximum standard deviation of average thickness is 2.33 m, and the maximum average temperature is 2.25 °C. For the autocorrelation function, the most significant impact comes from DBIN. For the coefficient of variation, the most significant impact comes from thermal conductivity. Different variations of hydrothermal parameters have different effects on the standard deviation of soft clay rock temperature. The biggest influence is the thermal conductivity, while the lowest influence is the specific heat capacity.

Keywords: soft clay rock; uncertain thermodynamic properties; stochastic analysis method; spatial variability; influencing factor

Citation: Wang, T.; Lin, H.; Ren, K.; Gao, J.; Wang, D. Sensitivity Analysis of Different Hydrothermal Characteristics in the Variable Thermodynamic Processes of Soft Clay Rock. *Appl. Sci.* **2024**, *14*, 10253. https://doi.org/10.3390/app142210253

Academic Editor: Fernando Rocha

Received: 19 September 2024
Revised: 5 November 2024
Accepted: 6 November 2024
Published: 7 November 2024

1. Introduction

In the underground space resources development within highly permeable and weakly consolidated formations, sustainable hazards often arise. These include groundwater inundation, leading to tunnel flooding and potential structural instability, soil subsidence due to water seepage, risking tunnel collapse, and environmental impacts like land settlement and groundwater contamination [1–3]. Addressing these challenges requires comprehensive engineering solutions, including artificial ground freezing, soil stabilization techniques, and effective groundwater management strategies, to ensure the sustainable and safe development of underground space in such geological conditions [4–6]. Artificial ground freezing (AGF) is a sophisticated engineering method extensively employed in underground space resources development. The freezing tube temperature can be reduced to −30 °C. The soil

temperature can be lowered to −15 °C. The permeability can be reduced by about three times. The strength can be increased by about three times. By manipulating groundwater levels and soil temperatures, AGF creates a protective frozen barrier underground, effectively shielding underground space excavation sites from water and soil infiltration [7,8]. This technique is particularly invaluable in areas with complex geological compositions and high groundwater levels, where traditional construction methods are prone to safety hazards like ground settlement and underground space collapse due to water seepage. AGF involves a series of meticulously executed steps, including pre-freezing to lower groundwater temperatures, primary freezing utilizing freezing pipes, and subsequent underground space excavation within the frozen support layer. Post-freezing curing is then carried out to ensure the long-term stability and integrity of the frozen barrier [9]. AGF not only guarantees high safety standards by mitigating the risks associated with groundwater ingress but also enhances construction efficiency by enabling uninterrupted excavation processes. Furthermore, its minimal environmental impact compared to conventional support structures underscores its significance in sustainable urban development initiatives. The temperature of underground space construction is crucial for ensuring the effectiveness and safety of AGF techniques [10]. It directly influences the formation and stability of the frozen barrier underground, which is essential for controlling groundwater inflow and stabilizing surrounding soil during excavation. By studying the optimal freezing temperature, engineers can enhance the efficiency of this method, minimize construction risks such as underground space collapse and ground settlement, and ultimately ensure the long-term structural integrity and safety of underground space [11,12].

The temperature field of the soft clay rock in underground space resources development is influenced by several factors. Firstly, the properties of the surrounding soft clay rock, such as thermal conductivity and moisture content, impact heat transfer rates and the extent of freezing. Secondly, the type and temperature of the refrigerant used for ground freezing play a critical role in controlling the temperature distribution within the soft clay rock. Additionally, environmental factors like ambient temperature and groundwater flow rates can affect the effectiveness of the freezing process. Furthermore, the geometry and design of the freezing system, including the spacing and arrangement of freezing pipes, also influence the temperature field [13–15]. Soft clay rock thermal conductivity determines the rate of heat transfer within the ground, impacting the freezing process's efficiency and the uniformity of temperature distribution in the underground space. Additionally, the moisture content of soft clay rock affects thermal conductivity and heat capacity, influencing the heat absorption and release capabilities. The permeability coefficient of soft clay rock governs the flow of groundwater, which can affect the effectiveness of ground freezing by influencing the distribution and stability of the frozen barrier [16,17]. The horizontal fluctuation range of clay rock is generally about 5 m, and the vertical fluctuation range is generally about 2 m. Variations in mineral composition, organic content, and moisture distribution lead to differences in thermal conductivity and heat capacity across soil layers. Similarly, variations in pore size, shape, and connectivity influence permeability coefficients, affecting the movement of fluids within the soft clay rock. Geological factors such as fractures, faults, and bedding planes further contribute to spatial heterogeneity in soft clay rock properties [18–20]. The mechanism behind quantifying spatial variability in geotechnical properties through stochastic field methods lies in capturing the inherent randomness and spatial correlation of geotechnical attributes [21,22]. These methods utilize statistical techniques to model the spatial distribution of soft clay rock parameters, considering factors such as geological heterogeneity, depositional processes, and environmental influences. By characterizing the spatial dependence structure of geotechnical properties, stochastic field approaches provide insights into the underlying processes governing variability across landscapes [23,24]. This includes accounting for factors such as soil texture, moisture content, and compaction, which influence the spatial distribution of properties like permeability, porosity, and shear strength [25,26]. Hence, the spatial variability of

hydrothermal parameters needs to be clarified, and the effects of variable hydrothermal parameters on the thermodynamic properties of soft clay rock need to be evaluated.

In this paper, the anisotropic spatial variations of the hydrothermal parameters of soft clay rock are counted by test data results. The statistical variability characteristics of variable hydrothermal parameters are estimated. A stochastic coupling model of thermodynamic characteristics for soft clay rock is proposed, and the uncertain temperature properties of underground space are computed. The reliability of the model is verified by test results. According to the relationship between anisotropic spatial variations and statistical variability characteristics for the different random field correlation models, the effects of autocorrelation function (ACF), coefficient of variation (COV), and autocorrelation distance (ACD) of variable hydrothermal parameter on the uncertain thermodynamic properties of soft clay rock are discussed. The results can provide a basis for the sustainable development of underground space.

2. Spatial Variability of Hydrothermal Parameter

The thermodynamic parameters of soft clay rock in underground space resource development are paramount for successful construction in soft clay rock layers. Ground freezing techniques rely on precise control of parameters like freezing temperature, freezing rate, and latent heat of fusion. These parameters dictate the extent and stability of frozen zones around underground space excavations, ensuring temporary ground support, preventing groundwater ingress, and minimizing settlement risks [27]. A thorough understanding and accurate management of thermodynamic parameters are crucial for maintaining underground space stability, protecting surrounding structures, and ensuring worker safety during construction. Improper control or deviation from optimal parameters can lead to ground instability, structural damage, and delays in project completion [28,29]. Therefore, meticulous attention to thermodynamic parameters is essential for the efficient and safe execution of underground space projects in soft clay rock formations.

2.1. Anisotropic Spatial Variations

The spatial variability of soft clay rock exhibits significant anisotropy, characterized by distinct directional variations in geotechnical properties. This anisotropy arises due to the orientation and arrangement of clay particles, which are influenced by factors such as sedimentation processes, depositional history, and mechanical loading conditions. In soft clay rock, the arrangement of clay particles tends to align along the principal stress directions, resulting in anisotropic behaviors in terms of strength, stiffness, and permeability. Moreover, the presence of soil structure and fabric further enhances the directional dependence of geotechnical properties. For instance, the orientation of clay platelets and micro-fabrics within the soil matrix can lead to pronounced variations in shear strength along different directions. Additionally, external factors such as loading history and environmental conditions can induce changes in the anisotropic behavior of soft clay rock over time. Understanding and characterizing the spatial variability and anisotropy of soft clay rock is essential for AGF applications [30–32]. In this study, the project background of this paper is that the section from Mengcheng Road Station to North Second Ring Road station of Hefei Rail Transit Line 5 is about 979 m long, the section roof is about 9.7~18.5 m, and the section floor is about 15.7~24.5 m buried. The shield method is intended to be used for construction; the tunnel diameter is about 6 m, and the formation constructed by the freezing method is soft clay rock. A series of soft clay rocks were collected, and thermodynamic tests were carried out. The range of DSC is 0~ ±500 mW, the temperature range is from −60 °C to 200 °C, the heating rate and cooling rates are 1~80 °C/min and 1~20 °C/min, respectively, the temperature resolution is 0.1 °C, the temperature fluctuation and repeatability are ±0.1 °C, the noise is 0.01 μW, the resolution and accuracy are 0.01 μW and 0.1 μW. The sensitivity is 0.1 μW. Our DSC equipment comes from Germany. A known temperature difference is applied across a sample of clay, and the rate of heat transfer is measured. By calculating the heat flux and knowing the geometry of the sample, the thermal

conductivity can be determined. Differentiating scanning calorimetry was used to measure the specific heat capacity. The sample is subjected to controlled temperature changes, and the heat flow into or out of the sample is measured. By analyzing the heat flow data, the specific heat capacity of the soft clay rock can be determined. The permeameter was used to assess the permeability. The constant head test is used in this paper. The inner diameter of the metal sealing cylinder, metal orifice plate, filter screen, pressure measuring pipe, and metal cylinder for the water supply bottle is 10 cm, and the height is 40 cm. The clay sample is placed in a permeameter cell, and water is allowed to flow through it under controlled conditions. By measuring the flow rate and applying Darcy's law, the permeability of the clay can be calculated. The depth of the soil sample was 10 m, and 10 sets of samples were obtained. The test results of the hydrothermal parameters of soft clay rock for ten different sampling points are shown in Figure 1. It can be seen that the discrete features are very evident because of the heterogeneity of the soft clay rock. The relationship between spatial variation in anisotropy and heterogeneous characteristics of soft clay rock is significant. Soft clay rock exhibits anisotropic behavior due to variations in its mineral composition, fabric orientation, and depositional history. These variations lead to spatial heterogeneity in properties such as permeability, compressibility, and thermophysical properties. The alignment of clay particles along certain directions can result in preferential pathways for fluid flow, causing anisotropic permeability. Additionally, localized concentrations of specific minerals or organic matter can create heterogeneities in thermodynamic behavior. Therefore, it is essential to analyze the statistical characteristics and variability of these data.

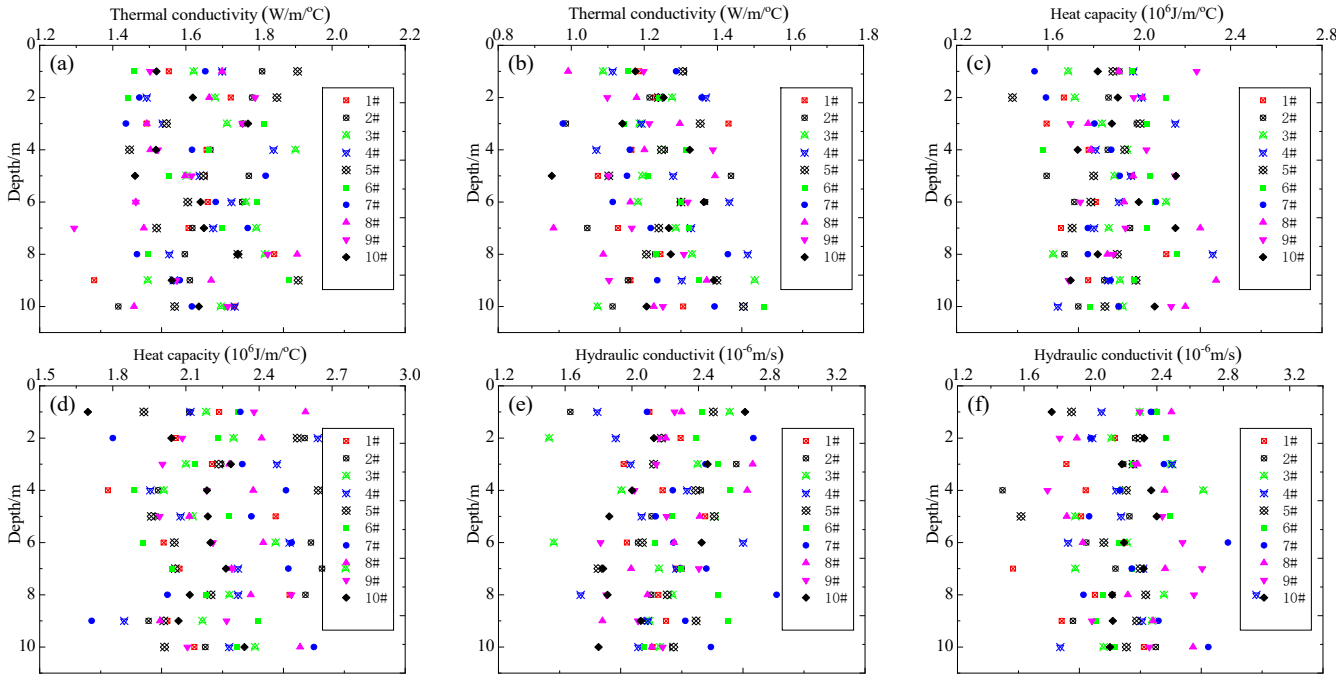

Figure 1. Hydrothermal parameter for 10 different sampling points: (**a**) Thermal conductivity of frozen state, (**b**) thermal conductivity of unfrozen state, (**c**) heat capacity of frozen state, (**d**) heat capacity of unfrozen state, (**e**) hydraulic conductivity of horizontal direction, (**f**) hydraulic conductivity of vertical direction.

2.2. Statistical Distribution Characteristics

The results of thermodynamic parameter testing for soft clay rock reveal a distinct statistical distribution pattern, highlighting the inherent variability in clay properties. Factors such as mineral composition, pore structure, and moisture content contribute to this variability, leading to diverse values of hydrothermal parameters. Rather than displaying a singular fixed value, these parameters exhibit a range of values distributed probabilistically. This statistical distribution reflects the heterogeneous nature of soft clay rock, where differ-

ent regions within a sample may possess varying properties [33,34]. Understanding this statistical distribution is essential for accurate modeling and prediction of clay behavior in engineering applications, as it allows for the incorporation of uncertainty and variability into predictive models. Advanced statistical techniques are often employed to analyze and interpret these results, providing valuable insights into the spatial variability and complexity of soft clay rock. Recognizing the statistical distribution of thermodynamic parameters in clay enhances our understanding of its behavior and facilitates more informed decision-making in engineering and environmental contexts. Based on the test results of the hydrothermal parameters of soft clay rock for ten different sampling points, the statistical value was calculated. The results are shown in Figure 2. For the thermal conductivity of the frozen state, the maximum is 1.907 W/m/°C while the minimum is 1.294 W/m/°C. The mean and standard deviation (SD) are 1.640 W/m/°C and 0.134 W/m/°C, respectively. For the thermal conductivity of the unfrozen state, the maximum is 1.526 W/m/°C while the minimum is 0.947 W/m/°C. The mean and SD are 1.241 W/m/°C and 0.124 W/m/°C, respectively. For the heat capacity of the frozen state, the maximum is 2.336×10^6 J/m^3/°C while the minimum is 1.445×10^6 J/m^3/°C. Mean and SD are 1.893×10^6 J/m^3/°C and 0.1764×10^6 J/m^3/°C, respectively. For the heat capacity of the unfrozen state, the maximum is 2.755×10^6 J/m^3/°C while the minimum is 1.697×10^6 J/m^3/°C. Mean and SD are 2.227×10^6 J/m^3/°C and 0.230×10^6 J/m^3/°C, respectively. For the hydraulic conductivity of horizontal direction, the maximum is 2.869×10^{-6} m/s, while the minimum is 1.504×10^{-6} m/s. Mean and SD are 2.203×10^{-6} m/s and 0.266×10^{-6} m/s, respectively. For the hydraulic conductivity of vertical direction, the maximum is 2.999×10^{-6} m/s while the minimum is 1.471×10^{-6} m/s. Mean and SD are 2.204×10^{-6} m/s and 0.265×10^{-6} m/s, respectively. It can be seen that the statistical distribution characteristics of hydraulic conductivity in the horizontal direction and vertical direction are approximate. Thus, it can be concluded that the permeability of soft clay rock in different directions is the same. In general, the statistical characteristics of the hydrothermal parameters show a normal distribution.

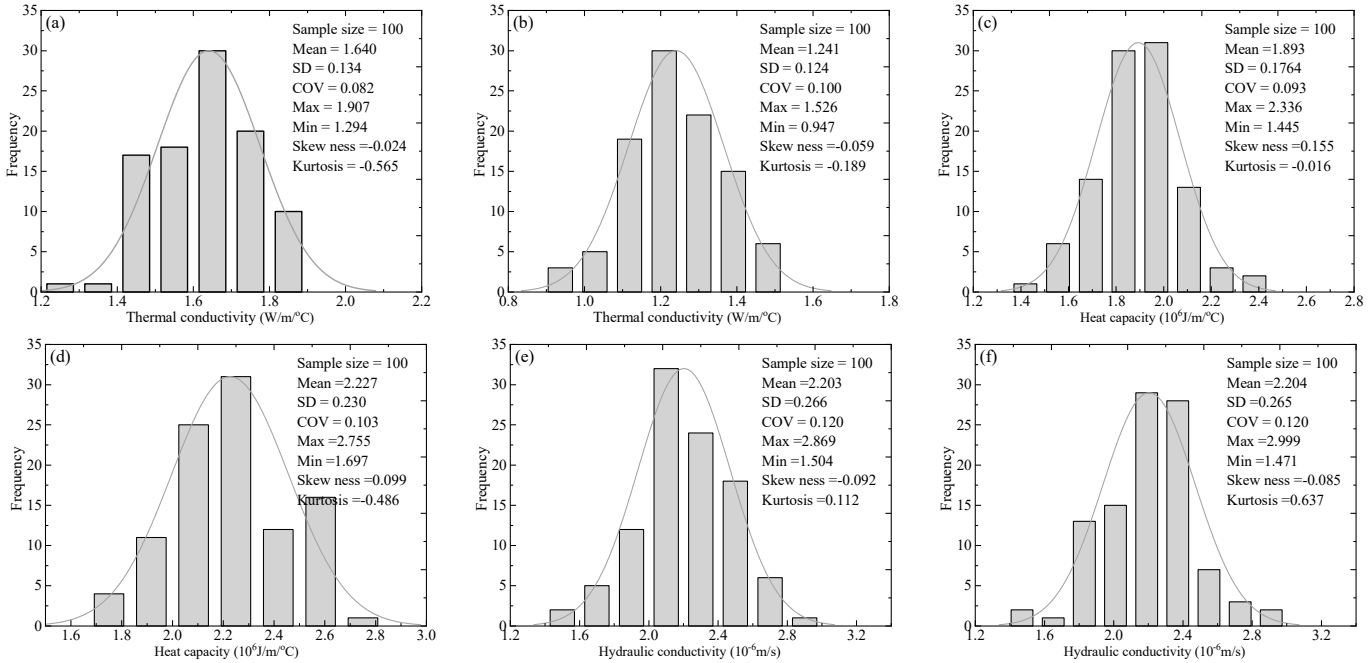

Figure 2. Statistical characteristics of hydrothermal properties: (**a**) Thermal conductivity of frozen state, (**b**) thermal conductivity of unfrozen state, (**c**) heat capacity of frozen state, (**d**) heat capacity of unfrozen state, (**e**) hydraulic conductivity of horizontal direction, (**f**) hydraulic conductivity of vertical direction.

2.3. Variability Distribution Characteristics

The spatial variability of thermodynamic parameters in soft clay rock is caused by a complex interplay of several underlying mechanisms. One primary factor contributing to this variability is the heterogeneous nature of clay at both micro and macro scales. At the microscale, clay minerals exhibit intricate structures and compositions, resulting in variations in thermal properties such as thermal conductivity and specific heat capacity. Variations in mineral composition, including the presence of different types of clay minerals and accessory minerals, can significantly influence thermal conductivity. Additionally, the arrangement of clay particles and their orientation within the clay matrix can create anisotropic behavior, further contributing to spatial variability. At the macroscale, geological processes such as sedimentation, weathering, and diagenesis play a crucial role in shaping the spatial distribution of clay properties. Variations in depositional environments, including factors like sedimentary facies and depositional conditions, can lead to spatial heterogeneity in clay properties across different geological formations. Furthermore, post-depositional processes such as compaction, cementation, and deformation can further modify the spatial distribution of soft clay rock properties, introducing additional variability. Environmental factors also influence the spatial variability of thermodynamic parameters. Variations in moisture content, temperature gradients, and chemical composition of pore fluids can affect thermal conductivity and specific heat capacity. Additionally, hydraulic gradients and flow pathways within clay formations can lead to preferential fluid flow and transport, influencing permeability distribution [35,36]. The spatial variability of clay thermodynamic parameters is further influenced by scale-dependent phenomena. At smaller scales, such as the pore scale, interactions between clay particles, pore fluid properties, and surface chemistry play a significant role in determining thermal and hydraulic properties. At larger scales, geological heterogeneity, structural features, and boundary conditions become more pronounced, influencing the overall spatial distribution of clay properties. Therefore, the spatial variability of thermodynamic parameters in soft clay rock is governed by a combination of factors, including mineralogical composition, geological processes, environmental conditions, and scale-dependent phenomena. Understanding these mechanisms is essential for accurately characterizing and predicting the behavior of soft clay rock in various engineering and environmental applications. Based on test data and random field theory, the COV, scale of fluctuation (SOF), and ACD can be calculated. The variability results of hydrothermal parameters are shown in Table 1.

Table 1. Variability of the hydrothermal parameters for the soft clay rock.

NO.	Thermal Conductivity				Heat Capacity				Hydraulic Conductivity			
	Frozen State		Unfrozen State		Frozen State		Unfrozen State		Horizontal Direction		Vertical Direction	
	COV	SOF	COV	SOF	COV	SOF	COV	SOF	COV	SOF	COV	SOF
1#	0.19	1.84	0.12	2.63	0.24	3.34	0.14	1.65	0.12	3.17	0.14	2.32
2#	0.23	2.38	0.18	2.32	0.13	2.75	0.14	1.99	0.16	3.48	0.17	2.84
3#	0.20	2.09	0.15	3.02	0.12	2.52	0.12	1.91	0.17	2.21	0.14	1.89
4#	0.09	2.56	0.18	1.81	0.18	3.60	0.12	1.73	0.15	3.05	0.15	3.53
5#	0.16	1.61	0.21	1.94	0.22	2.39	0.13	2.16	0.17	2.81	0.13	2.47
6#	0.20	2.32	0.18	3.60	0.19	3.27	0.10	1.49	0.08	2.10	0.13	1.66
7#	0.10	1.48	0.14	2.87	0.18	2.55	0.15	2.25	0.15	2.73	0.18	2.90
8#	0.16	1.48	0.19	3.50	0.15	3.26	0.14	1.27	0.16	2.75	0.18	3.70
9#	0.19	2.24	0.14	2.70	0.13	3.31	0.14	2.36	0.17	2.25	0.11	2.91
10#	0.07	2.03	0.13	2.91	0.17	2.38	0.05	2.32	0.16	1.70	0.12	2.96

Random field theory is a powerful framework for characterizing the spatial variability of hydrothermal parameters [37]. In this theory, soft clay rock properties are treated as random fields, exhibiting inherent variability across space. The essence of this approach lies in recognizing that soft clay rock properties vary stochastically due to diverse geological

processes, environmental influences, and heterogeneity in soil composition and structure. By representing soft clay rock parameters as random fields, stochastic field theory captures the complex and nonlinear spatial patterns of variability observed in soft clay rock properties. Statistical descriptors such as mean, variance, and spatial correlation length are used to quantify the average behavior, degree of variability, and spatial dependence of soft clay rock parameters, respectively. Variogram analysis is often employed to characterize the spatial correlation structure, providing insights into the range over which parameter values exhibit spatial correlation. Through stochastic field theory, spatial realizations of soil parameter fields can be generated, simulating multiple plausible spatial distributions of parameters. Based on the variability results of the hydrothermal parameters and random field, the COV, SOF, and ACD can be obtained. The variability distribution characteristics of the hydrothermal parameters for the soft clay rock are shown in Figure 3. The observation reveals that the COV varies between 0.05 and 0.25, the SOF varies between 1.2 m and 4.0 m, and the ACD varies between 0.4 m and 1.4 m, respectively.

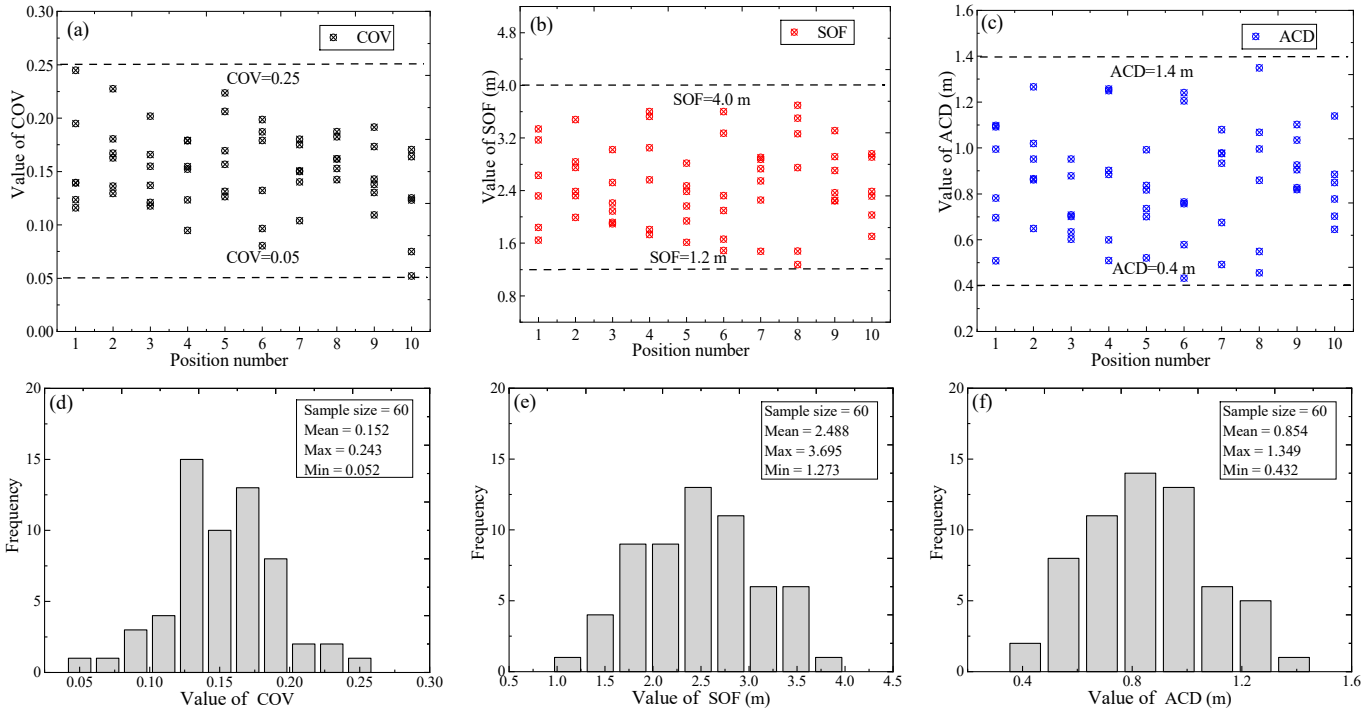

Figure 3. Variability characteristics of hydrothermal properties: (**a**) Discrete distribution of COV, (**b**) discrete distribution of SOF, (**c**) discrete distribution of ACD, (**d**) statistical characteristics of COV, (**e**) statistical characteristics of SOF, (**f**) statistical characteristics of ACD.

3. Uncertain Analysis Method of Thermodynamic Properties

3.1. Coupled Governing Equations

The mechanism of temperature-permeability coupling in frozen soft clay rock elucidates the intricate interplay between thermal dynamics and fluid flow. At its core, the mechanism involves the manipulation of temperature to induce freezing in rock pores, altering their permeability and hydraulic conductivity. As temperature decreases, pore water freezes, leading to a reduction in pore size and an increase in rock matrix strength. Consequently, the permeability of the soft clay rock decreases, restricting fluid flow. However, the coupling is not solely determined by temperature. Factors such as ice formation rate, soil composition, and boundary conditions also influence the process. Understanding this mechanism is critical for optimizing freezing techniques, designing effective containment systems, and predicting the behavior of soft clay rock under various conditions. By comprehending the temperature-permeability coupling mechanism in underground space, engineers can develop sustainable solutions for infrastructure development in cold regions,

mitigate environmental impacts, and ensure the long-term stability of engineered structures in frozen soft clay rock environments [38]. The coupled equations can be expressed as follows:

In the frozen area Ω_{f}:

$$C_{\mathrm{f}}\frac{\partial T_{\mathrm{f}}}{\partial t} = \frac{\partial}{\partial x}\left(\lambda_{\mathrm{f}}\frac{\partial T_{\mathrm{f}}}{\partial x}\right) + \frac{\partial}{\partial y}\left(\lambda_{\mathrm{f}}\frac{\partial T_{\mathrm{f}}}{\partial y}\right) - C_w\rho_w\left(V_x^{\mathrm{f}}\frac{\partial T_{\mathrm{f}}}{\partial x} + V_y^{\mathrm{f}}\frac{\partial T_{\mathrm{f}}}{\partial y}\right) \tag{1}$$

$$S_{\mathrm{f}}\frac{\partial H_{\mathrm{f}}}{\partial t} = \frac{\partial}{\partial x}\left(K_x^{\mathrm{f}}\frac{\partial H_{\mathrm{f}}}{\partial x}\right) + \frac{\partial}{\partial \mathrm{y}}\left(K_y^{\mathrm{f}}\frac{\partial H_{\mathrm{f}}}{\partial y}\right) + Q \tag{2}$$

$$V_x^{\mathrm{f}} = -K_x^{\mathrm{f}}\frac{\partial H_{\mathrm{f}}}{\partial x},\ V_y^{\mathrm{f}} = -K_y^{\mathrm{f}}\frac{\partial H_{\mathrm{f}}}{\partial y} \tag{3}$$

In the unfrozen area Ω_{u}:

$$C_{\mathrm{u}}\frac{\partial T_{\mathrm{u}}}{\partial t} = \frac{\partial}{\partial x}\left(\lambda_{\mathrm{u}}\frac{\partial T_{\mathrm{u}}}{\partial x}\right) + \frac{\partial}{\partial y}\left(\lambda_{\mathrm{u}}\frac{\partial T_{\mathrm{u}}}{\partial y}\right) - C_w\rho_w\left(V_x^{\mathrm{u}}\frac{\partial T_{\mathrm{u}}}{\partial x} + V_y^{\mathrm{u}}\frac{\partial T_{\mathrm{u}}}{\partial y}\right) \tag{4}$$

$$S_{\mathrm{u}}\frac{\partial H_{\mathrm{u}}}{\partial t} = \frac{\partial}{\partial x}\left(K_x^{\mathrm{u}}\frac{\partial H_{\mathrm{u}}}{\partial x}\right) + \frac{\partial}{\partial y}\left(K_y^{\mathrm{u}}\frac{\partial H_{\mathrm{u}}}{\partial y}\right) + Q \tag{5}$$

$$V_x^{\mathrm{u}} = -K_x^{\mathrm{u}}\frac{\partial H_{\mathrm{u}}}{\partial x},\ V_y^{\mathrm{u}} = -K_y^{\mathrm{u}}\frac{\partial H_{\mathrm{u}}}{\partial y} \tag{6}$$

In Equations (1)–(6), f and u represent the frozen and the unfrozen states, respectively. T_{f}, C_{f}, and λ_{f} are the temperature, volumetric heat capacity, and thermal conductivity of foundation soils in the frozen area Ω_{f}, respectively. H_{f}, S_{f}, K_x^f and K_y^f are the water head, specific yield, and permeability coefficients in the frozen area Ω_{f}, respectively. Q is the source or collection of the seepage field. Variables V_x and V_y are the seepage rates in the x and y directions, respectively. C_w and ρ_w are the volumetric heat capacity and bulk density of water. Parameters with subscript u are the corresponding physical components in the unfrozen area Ω_{u}. t is time, and x, y are distances.

At the freezing-front position s ($\boldsymbol{x}$;t), in which $\boldsymbol{x}$ = {x, y}, The following equation needs to be satisfied.

$$T_{\mathrm{f}}(s(\boldsymbol{x},t),t) = T_{\mathrm{u}}(s(\boldsymbol{x},t),t) = T_{\mathrm{m}} \tag{7}$$

$$\lambda_{\mathrm{f}}\frac{\partial T_{\mathrm{f}}}{\partial n} - \lambda_{\mathrm{u}}\frac{\partial T_{\mathrm{u}}}{\partial n} = L\frac{\mathrm{d}s(\boldsymbol{x},t)}{\mathrm{d}t} \tag{8}$$

where L is the latent heat per unit volume, n is the direction vector of the moving boundary s ($\boldsymbol{x}$;t), and T_{m} is the phase change temperature.

The hydrothermal parameters can be expressed as

$$C^* = \begin{cases} C_{\mathrm{f}} & T < T_{\mathrm{m}} - \Delta T \\ \frac{C_{\mathrm{u}}+C_{\mathrm{f}}}{2} + \frac{L}{2\Delta T} & T_{\mathrm{m}} - \Delta T \le T \le T_{\mathrm{m}} + \Delta T_{\mathrm{u}} \\ C_{\mathrm{u}} & T > T_{\mathrm{m}} + \Delta T_{\mathrm{u}} \end{cases} \tag{9}$$

$$\lambda^* = \begin{cases} \lambda_{\mathrm{f}} & T < T_{\mathrm{m}} - \Delta T \\ \lambda_{\mathrm{f}} + \frac{\lambda_{\mathrm{u}}-\lambda_{\mathrm{f}}}{2\Delta T}[T - (T_{\mathrm{m}} - \Delta T)] & T_{\mathrm{m}} - \Delta T \le T \le T_{\mathrm{m}} + \Delta T \\ \lambda_{\mathrm{u}} & T > T_{\mathrm{m}} + \Delta T \end{cases} \tag{10}$$

The hydraulic conductivity can be written as follows:

$$K_x^* = \begin{cases} \left(\frac{W_{\mathrm{u}}}{W}\right)^{\beta}\cdot K_x^{\mathrm{u}} & T \le T_{\mathrm{m}} \\ K_x^{\mathrm{u}} & T > T_{\mathrm{m}} \end{cases},\ K_y^* = \begin{cases} \left(\frac{W_{\mathrm{u}}}{W}\right)^{\beta}\cdot K_y^{\mathrm{u}} & T \le T_{\mathrm{m}} \\ K_y^{\mathrm{u}} & T > T_{\mathrm{m}} \end{cases} \tag{11}$$

where W and W_{u} denote the water content and unfrozen water content of soil, respectively. The constant β is determined experimentally.

Using Equations (9)–(11), Equations. (1)–(8) can be written simply as

$$C^* \frac{\partial T}{\partial t} = \frac{\partial}{\partial x}\left(\lambda^* \frac{\partial T}{\partial x}\right) + \frac{\partial}{\partial y}\left(\lambda^* \frac{\partial T}{\partial y}\right) - C_w \rho_w \left(V_x^* \frac{\partial T}{\partial x} + V_y^* \frac{\partial T}{\partial y}\right) \tag{12}$$

$$S^* \frac{\partial H}{\partial t} = \frac{\partial}{\partial x}\left(K_x^* \frac{\partial H}{\partial x}\right) + \frac{\partial}{\partial y}\left(K_y^* \frac{\partial H}{\partial y}\right) + Q \tag{13}$$

where

$$S^* = \begin{cases} S_\mathrm{f} & T \le T_\mathrm{m} \\ S_\mathrm{u} & T > T_\mathrm{m} \end{cases} \tag{14}$$

$$V_x^* = -K_x^* \frac{\partial H}{\partial x},\ V_y^* = -K_y^* \frac{\partial H}{\partial y} \tag{15}$$

3.2. Uncertainty Characterization Method

The principle behind quantifying soft clay rock parameter uncertainty in spatial random fields lies in understanding and modeling the inherent spatial variability of soft clay rock properties. Geotechnical parameters, such as permeability, porosity, and shear strength, exhibit spatial heterogeneity due to geological processes, depositional patterns, and environmental factors. Spatial random field theory provides a framework to represent this variability by characterizing the statistical properties of geotechnical parameters across a given area. This involves analyzing spatial autocorrelation structures using tools like variograms and covariance functions. Geostatistical techniques, including kriging and stochastic simulation, are then employed to interpolate or simulate geotechnical parameters, accounting for spatial dependency and uncertainty. The local averaging method in random fields, also known as the moving window technique, is a powerful approach used in geostatistics and spatial analysis to simulate spatially correlated data. This method involves partitioning a random field into a series of overlapping windows and computing the local average within each window. The process begins by defining a window size and shape, typically a square or circular area, and then moving this window across the field, calculating the average of the data points within each window. The center of the window is then assigned the average value obtained. This process is repeated for each window, resulting in a new simulated field with spatially correlated values. The local averaging method offers several advantages, including simplicity, computational efficiency, and the ability to preserve local spatial patterns [39,40]. It is particularly useful for simulating spatially correlated phenomena with complex spatial structures, such as geotechnical properties, groundwater levels, or geological formations. Parameterization of the local averaging method involves determining the appropriate window size and shape based on the spatial characteristics of the data and the desired level of spatial correlation. The choice of parameters can significantly impact the simulated results, with larger windows capturing broader spatial trends and smaller windows preserving finer-scale variability. To optimize parameters, practitioners often employ cross-validation techniques or sensitivity analyses to assess the performance of different parameter combinations. By adjusting the parameters and comparing the simulated results to observed data or known spatial patterns, the most suitable parameter values can be identified for a given application. The three hydrothermal parameters of the freezing curtain are simulated as three two-dimensional random fields. It can be expressed as follows:

$$X_e = \frac{1}{A_e} \int_{\Omega_e} X(x, y) dx dy \tag{16}$$

The covariance can be expressed as

$$Cov(X_e, X_{e'}) = \frac{\sigma^2}{A_e A_{e'}} \sum_{i=1}^{4} \sum_{j=1}^{4} \sum_{m=1}^{4} \sum_{l=1}^{4} H_i H_j H_m H_l \rho(\Delta x, \Delta y) |J| \left|J'\right| \tag{17}$$

where A_e is the area of e; $A_{e'}$ is the area of e'; H_i, H_j, H_m, and H_l are the weighting coefficients; ρ (Δx, Δy) is the correlation structure of original random field; $|J|$ and $|J'|$ are the Jacobian determinants of coordinate transformation.

It can be seen that the covariance can be calculated as long as ρ (Δx, Δy) is given. The autocorrelation function in stochastic fields quantifies the degree of similarity between a random variable and a lagged version of itself across space or time. It is a fundamental tool in analyzing spatial or temporal dependence patterns within stochastic processes. The autocorrelation function describes how the correlation between points changes as the distance between them varies. For example, in spatial applications, the autocorrelation function often exhibits decay with increasing distance, indicating a diminishing correlation between points farther apart. Various mathematical forms can represent the autocorrelation function, such as exponential, Gaussian, or spherical models, each suited to different spatial or temporal contexts. Understanding and accurately modeling the autocorrelation function are crucial for tasks like spatial interpolation, prediction, and simulation within stochastic field analysis. In this study, the symbols θ_x and θ_y are used to represent horizontal ACD and vertical ACD. The symbols δ_x and δ_y are used to represent horizontal and vertical SOF. The mathematical expressions and parametric relationships of five common autocorrelation functions are shown in Table 2. Five kinds of two-dimensional random fields have different related structures, and the parameter relationships between SOF and ACD are different.

Table 2. Autocorrelation functions for characterizing the spatial variability of hydrothermal properties.

Name	Autocorrelation Functions	Parameter Relationship
DSNX	$\rho(\boldsymbol{\tau}) = \exp\left[-\left(\frac{\Delta x}{\theta_x} + \frac{\Delta y}{\theta_y}\right)\right]$	$\theta_x = \frac{\delta_x}{2}, \theta_y = \frac{\delta_y}{2}$
DSQX	$\rho(\boldsymbol{\tau}) = \exp\left\{-\left[\left(\frac{\Delta x}{\theta_x}\right)^2 + \left(\frac{\Delta y}{\theta_y}\right)^2\right]\right\}$	$\theta_x = \frac{\delta_x}{\sqrt{\pi}}, \theta_y = \frac{\delta_y}{\sqrt{\pi}}$
DSMK	$\rho(\boldsymbol{\tau}) = \exp\left[-\left(\frac{\Delta x}{\theta_x} + \frac{\Delta y}{\theta_y}\right)\right]\left[\left(1 + \frac{\Delta x}{\theta_x}\right)\left(1 + \frac{\Delta y}{\theta_y}\right)\right]$	$\theta_x = \frac{\delta_x}{4}, \theta_y = \frac{\delta_y}{4}$
DCSX	$\rho(\boldsymbol{\tau}) = \exp\left[-\left(\frac{\Delta x}{\theta_x} + \frac{\Delta y}{\theta_y}\right)\right]\cos\left(\frac{\Delta x}{\theta_x}\right)\cos\left(\frac{\Delta y}{\theta_y}\right)$	$\theta_x = \delta_x, \theta_y = \delta_y$
DBIN	$\rho(\boldsymbol{\tau}) = \begin{cases} \left(1 - \frac{\Delta x}{\theta_x}\right)\left(1 - \frac{\Delta y}{\theta_y}\right) & \Delta x \le \theta_x, \Delta y \le \theta_y \\ 0 & \Delta x > \theta_x, \Delta y > \theta_y \end{cases}$	$\theta_x = \delta_x, \theta_y = \delta_y$

3.3. Hydrothermal Parameters and Boundary Conditions

Boundary and initial conditions significantly influence the thermal characteristics analysis of freeze curtains in underground space engineering. Boundary conditions dictate the exchange of heat between the soft clay rock and the surrounding environment, affecting temperature distribution and freeze front progression. Similarly, initial conditions determine the starting temperature profile within the ground, impacting the rate and extent of freezing. Accurate consideration of these conditions is vital for assessing the effectiveness of soft clay rock in controlling ground temperatures and preventing settlement during underground space construction [41]. Understanding their influence aids in optimizing underground space resource development design and operational parameters to ensure efficient heat extraction and ground stabilization. Moreover, it facilitates the prediction of potential thermal impacts on adjacent structures and utilities, enhancing safety and sustainability in underground infrastructure projects. According to the coupling equation of the soft clay rock, the content of unfrozen water in soft clay rock is an important index to evaluate the water transport characteristics, and it is also a common parameter in thermal calculation. The experimental fitting curve equation can be expressed as

$$W_u = \begin{cases} P|T|_Q & T \le T_\mathrm{m} \\ W & T > T_\mathrm{m} \end{cases} \tag{18}$$

Based on field test data, parameters P and Q are 0.348 and -0.172, respectively.

Water head boundary condition:

$$H = H_0 \tag{19}$$

Flow boundary condition:

$$K_x \frac{\partial H}{\partial x} \cos(n, x) + K_y \frac{\partial H}{\partial y} \cos(n, y) = -q_0 \tag{20}$$

Temperature conditions:

$$T(r_0, t) = T_c \tag{21}$$

$$T(\infty, t) = T_0 \tag{22}$$

where r_0 is outer diameter; T_c is surface temperature; T_0 is initial temperature.

Initial temperature conditions:

$$T(r, 0) = T_0 \tag{23}$$

In this paper, underground space engineering is implemented in soft clay rock layers with three rings of freezing pipes. The inner ring has a diameter of 3.5 m, the middle ring has a diameter of 4.1 m, and the outer ring has a diameter of 4.7 m. There are 18 freezing pipes in both the inner and middle rings, while the outer ring has 32 freezing pipes. The outer diameter of the freezing pipes, r_0, is 0.06 m, and the average surface temperature, Tc, is −30 °C. The initial temperature, T_0, of the ground soil is 25 °C. The water head, H_0, is about 1.5 m. From the spatial variability of the hydrothermal parameters of soft clay rock (Figures 2 and 3), the statistical distribution patterns and the range of variation of COV and ACD are known. Based on the uncertain analysis method, the effect of variable parameters on the uncertain thermodynamic properties of soft clay rock can be evaluated.

4. Results and Analyses

4.1. Verification of Stochastic Coupling Model

Validating analytical models for analyzing the thermal characteristics of soft clay rock in underground space engineering is essential for several reasons. Firstly, it ensures the reliability and accuracy of predictions concerning temperature distributions and the progression of the freezing front within the surrounding soil. Accurate predictions are critical for optimizing freeze designs and operational parameters to effectively control ground temperatures and prevent soil settlement during underground space engineering, ensuring the safety and stability of the infrastructure. Secondly, validation enables the assessment of the model's applicability across various geological and climatic conditions. Subsurface conditions can vary significantly from one location to another, and validating the model across different scenarios helps ensure its robustness and generalizability. Thirdly, the validation process helps identify any limitations or discrepancies between model predictions and real-world observations. This feedback loop guides improvements and refinements to the analytical model, enhancing its accuracy and reliability over time. Ultimately, validated analytical models serve as valuable tools for engineers and planners, providing insights into the thermal behavior of soft clay rock and supporting informed decision-making in underground space engineering. Points A, B, and C represent three sample points vertically spaced 1 m apart within the first ring of freezing pipes. Figure 4a shows the results of the experimental and numerical temperatures of soft clay rock for Points A, B, and C. From Figure 4a, it can be observed that the calculated mean temperature results of the uncertain analysis model of thermodynamic properties for the soft clay rock are close to the experimental results at Points A, B, and C. This is consistent with the law of large numbers in statistics, indicating that the Monte Carlo random simulation yields mean temperatures that are approximately equal to the statistically measured temperatures. As freezing time increases, the temperature of Points A, B, and C gradually decreases. When

the mean temperature approaches 0 °C, there is a noticeable plateau in the curve. This is due to the phase transition between ice and water, releasing latent heat, which slows down the cooling trend. Similarly, Points D, E, and F represent three sample points horizontally spaced 1 m apart within the first ring of freezing pipes. Figure 4b shows the results with the experimental temperatures and numerical temperatures of soft clay rock for Points D, E, and F. From Figure 4b, the calculated mean temperature results of the uncertain analysis model of thermodynamic properties for the soft clay rock are close to the experimental results at Points D, E, and F. This is consistent with the Law of Large Numbers in statistics, indicating that the average temperature generated by random simulation is approximately equal to the statistically measured temperature. As freezing time increases, the temperature of Points D, E, and F gradually decreases. When the mean temperature approaches 0 °C, there is a noticeable plateau in the curve. This is due to the phase transition between ice and water, releasing latent heat, which slows down the cooling trend. Therefore, the proposed stochastic analysis model for the thermal characteristics of soft clay rock, considering the spatial variability of variable hydrothermal parameters, is scientifically reasonable.

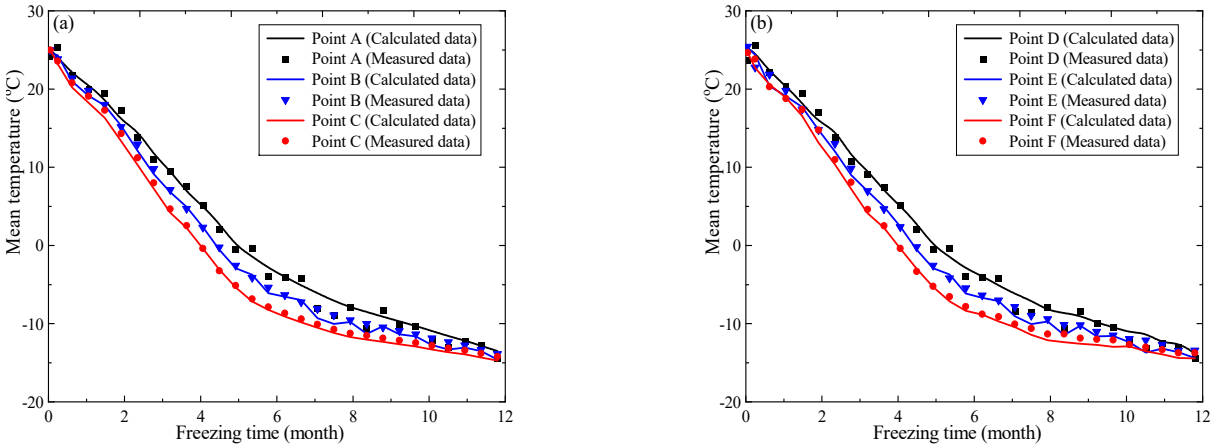

Figure 4. Experimental temperatures and numerical temperatures of soft clay rock: (**a**) measured data and calculated data of Points A, B, and C; (**b**) measured data and calculated data of Points D, E, and F.

4.2. Mean and SD of Thermodynamic Properties

Analyzing the evolution of average temperature and average thickness of soft clay rock in underground space engineering is crucial for several reasons. Firstly, it provides insights into the thermal behavior of the surrounding soft clay rock and the effectiveness of the soft clay rock in controlling ground temperatures. Understanding how the average temperature changes over time helps in optimizing freeze designs and operational parameters to ensure adequate ground freezing and prevent soil settlement during tunnel construction. Secondly, monitoring the average thickness evolution allows engineers to assess the progression of the freezing front within the soil. By tracking changes in thickness, they can identify potential areas of inadequate freezing and take corrective measures to enhance freeze-soft clay rock performance. Moreover, analyzing the evolution of both temperature and thickness provides valuable data for validating analytical models and simulation tools used in underground space engineering. Comparing model predictions with observed data enhances the accuracy and reliability of these tools, ultimately improving decision-making and risk management during underground space engineering. Furthermore, understanding the long-term evolution of average temperature and thickness helps in assessing the stability and durability of underground space engineering over time. By predicting how these parameters will evolve under different conditions, engineers can implement preventive maintenance measures and ensure the long-term integrity of underground space engineering. In summary, analyzing the evolution of average temperature and thickness of soft clay rock is essential for optimizing design, validating models, ensuring construction safety, and maintaining the long-term stability of underground infrastructure. Sections A, B, C, D,

and E represent five sections through the center of the inner ring of freezing pipes, with azimuth angles of 0°, 45°, 90°, 135°, and 180°, respectively. Figure 5 shows the variability of temperature characteristic value of soft clay rock. From Figure 5a, the overall trend of the average thickness of the soft clay rock increases with the increase of freezing time. From the second month to the 10th month, it increases at a faster rate, and there are differences in the thickness of different sections, with the largest difference being 1.35 m, which is due to the fact that the frozen curtain has not formed a stable form. When the freezing time reaches 12 months, the average thickness stabilizes, indicating that the stable formation of the frozen curtain is essentially achieved at this point. From Figure 5c, the overall trend of the average temperature of the frozen curtain decreases with the increase of freezing time. From the second month to the 10th month, it decreases at a relatively fast rate, and there are differences in the temperature of different sections, with the largest difference being 0.58 °C, which is due to the fact that the frozen curtain has not formed a stable form. When the freezing time reaches 12 months, the average temperature stabilizes, indicating that the stable formation of the frozen curtain is essentially achieved at this point. From Figure 5b,c, the overall trend of SD of the freeze curtain increases with time. When the freezing time reaches 12 months, the SD of the average thickness and temperature stabilizes.

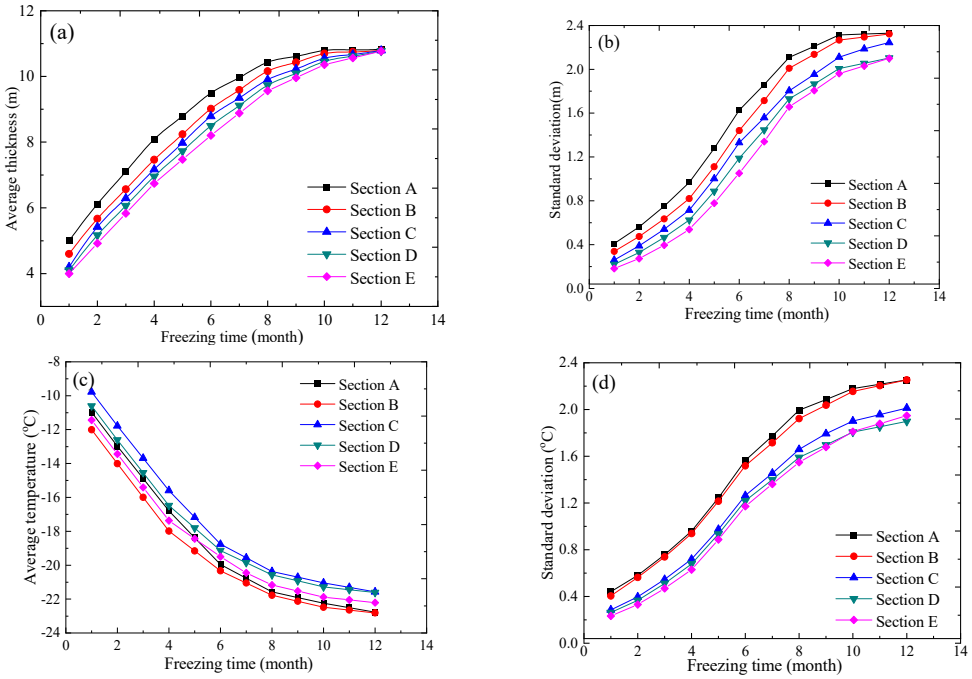

Figure 5. Variability of temperature characteristic value of soft clay rock: (**a**) Average thickness of freezing curtain; (**b**) standard deviation of average thickness; (**c**) average temperature of freezing curtain; (**d**) standard deviation of average temperature.

4.3. Effect of ACF on Hydrothermal Parameters

Evaluating the ACF of stochastic fields of hydrothermal parameters is crucial for understanding the impact on temperature distribution of soft clay rock in underground space engineering. The ACF characterizes the spatial dependency of hydrothermal parameters for the soft clay rock. This information is vital for predicting the spatial variation of temperature within the soil mass and, consequently, the performance of freeze curtains. By analyzing the autocorrelation function, engineers can assess how thermal properties vary over different distances within the soft clay rock. This understanding enables the estimation of the range at which thermal influences propagate, guiding the design and placement of freeze curtain elements for optimal temperature control. Additionally, it helps identify areas of high spatial variability where additional monitoring or intervention may be necessary to ensure uniform freezing and prevent ground settlement. Furthermore,

incorporating the ACF into thermal analysis models enhances their accuracy and reliability. By capturing the spatial correlation of thermal parameters, these models can provide more realistic predictions of temperature distributions within the soil mass and along the soft clay rock. This is essential for optimizing freeze curtain designs, ensuring adequate ground freezing, and minimizing the risk of soil instability during underground space engineering. Overall, evaluating the ACF of hydrothermal parameters is essential for understanding the spatial variability of temperature within underground space engineering environments. It facilitates informed decision-making in freeze curtain design and construction, ultimately ensuring the safety, stability, and longevity of underground infrastructure. To elucidate the ACF on the variability of temperature characteristics of frozen curtains, this paper selects the DSNX, DSQX, DSMK, DCSX, and DBIN models to represent the ACF of frozen soft clay rock layers and conducts sensitivity grouping (Table 3) calculations for correlation structure models. The results are shown in Figure 6.

Table 3. Parametric influence of different ACFs of hydrothermal properties.

Case ID	Thermal Conductivity		Heat Capacity		Hydraulic Conductivity	
	λ_u (W/m/°C)	λ_f (W/m/°C)	C_u (10^6 J/m^3/°C)	C_f (10^6 J/m^3/°C)	$K_x{}^u$ (10^{-6} m/s)	$K_y{}^u$ (10^{-6} m/s)
Reference case	DSQX	DSQX	DSQX	DSQX	DSQX	DSQX
ACF of thermal conductivity	DSNX	DSNX	DSQX	DSQX	DSQX	DSQX
	DSQX	DSQX	DSQX	DSQX	DSQX	DSQX
	DSMK	DSMK	DSQX	DSQX	DSQX	DSQX
	DCSX	DCSX	DSQX	DSQX	DSQX	DSQX
	DBIN	DBIN	DSQX	DSQX	DSQX	DSQX
ACF of heat capacity	DSQX	DSQX	DSNX	DSNX	DSQX	DSQX
	DSQX	DSQX	DSQX	DSQX	DSQX	DSQX
	DSQX	DSQX	DSMK	DSMK	DSQX	DSQX
	DSQX	DSQX	DCSX	DCSX	DSQX	DSQX
	DSQX	DSQX	DBIN	DBIN	DSQX	DSQX
ACF of hydraulic conductivity	DSQX	DSQX	DSQX	DSQX	DSNX	DSNX
	DSQX	DSQX	DSQX	DSQX	DSQX	DSQX
	DSQX	DSQX	DSQX	DSQX	DSMK	DSMK
	DSQX	DSQX	DSQX	DSQX	DCSX	DCSX
	DSQX	DSQX	DSQX	DSQX	DBIN	DBIN

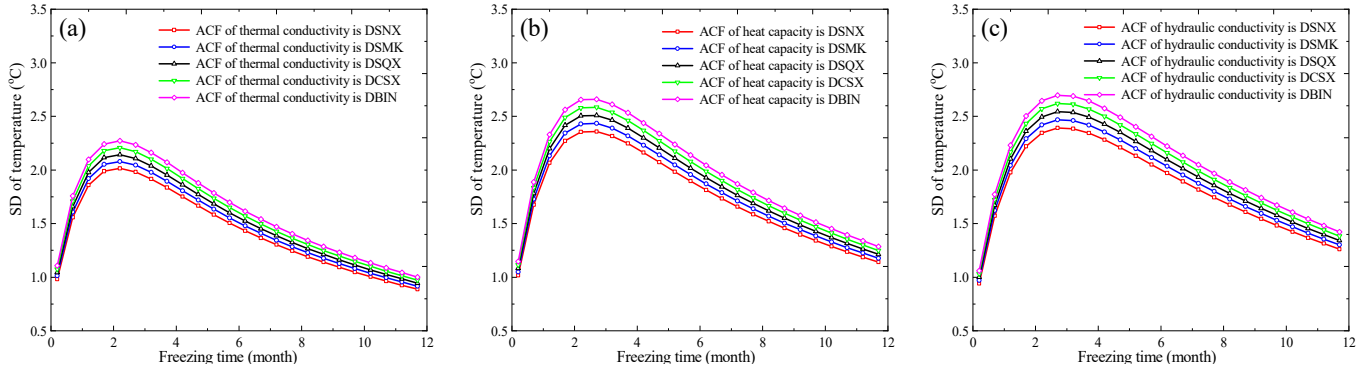

Figure 6. Effects of different ACFs of variable hydrothermal parameters on uncertain thermodynamic properties: (**a**) Thermal conductivity; (**b**) heat capacity; (**c**) hydraulic conductivity.

Figure 6 shows that the five different random field-related structures have different effects on the SD of freezing soft clay rock temperature. When DBIN is used, the SD of freezing curtain temperature is the largest. When DSQX is used, the SD of the freezing

curtain temperature is in the middle. When DSNX is used, the SD of the freezing curtain temperature is the smallest. For the thermal conductivity, the maximum and minimum SD of freezing curtain temperature during the freezing process are 2.27 °C and 0.89 °C, respectively. For the spatial variability of heat capacity, the maximum and minimum SD of freezing curtain temperature during the freezing process are 2.66 °C and 1.02 °C, respectively. For the hydraulic conductivity, the maximum and minimum SD of freezing curtain temperature during freezing is 2.70 °C and 0.94 °C, respectively. Therefore, different correlation functions have different variability effects on the freezing curtain temperature. The most significant impact comes from DBIN, followed by DSQX, with DSNX having the smallest effect.

4.4. Effect of COV of Hydrothermal Parameter

The COV of thermal parameters in soft clay rock plays a significant role in influencing the temperature distribution of freeze curtains. As the COV increases, it indicates greater variability or heterogeneity in thermal properties within the frozen soft clay rock. This variability directly affects the spatial distribution of temperature within the soil mass and along the freeze curtain. In regions with high COV values, there is greater uncertainty in thermal properties, leading to more pronounced temperature variations. This can result in non-uniform freezing along the freeze curtain, with some areas experiencing higher or lower temperatures than others. In contrast, lower COV values indicate more consistent thermal properties, resulting in a more uniform temperature distribution along the freeze curtain. Understanding the impact of COV on freeze curtain temperature is crucial for optimizing freeze curtain designs and ensuring effective ground stabilization during underground space engineering. Engineers can use this information to identify regions of high COV, where additional measures may be needed to achieve uniform freezing and prevent ground settlement. Additionally, incorporating COV data into thermal analysis models improves their accuracy and reliability, enabling better predictions of temperature distributions within the soft clay rock. Overall, the relationship between the COV of thermal parameters and freeze curtain temperature highlights the importance of considering spatial variability in thermal properties when designing and implementing freeze curtain systems in underground space engineering. By accounting for COV values, engineers can make informed decisions to enhance the safety, stability, and efficiency of underground infrastructure projects. To elucidate the effect of COV on the temperature characteristics of soft clay rock, this paper selects the 0.05, 0.10, 0.15, 0.20, and 0.25 to represent the COV of hydrothermal parameters and conducts sensitivity grouping (Table 4) calculations for parameter variability. The results are shown in Figure 7.

Figure 7 shows that the five different COVs have different effects on the SD of freezing temperature. For the thermal conductivity, When the COV is 0.05, the SD of the freezing curtain temperature is the smallest. When the COV is 0.15, the SD of the freezing curtain temperature is in the middle. When the COV is 0.25, the SD of the freezing curtain temperature is the largest. The maximum and minimum SD of freezing curtain temperature during the freezing process is 3.09 °C and 0.73 °C, respectively. For the heat capacity, When the COV is 0.05, the SD of the freezing curtain temperature is the smallest. When the COV is 0.15, the SD of the freezing curtain temperature is in the middle. When the COV is 0.25, the SD of the freezing curtain temperature is the largest. The maximum and minimum SD of the freezing curtain temperature during the freezing process are 1.91 °C and 0.59 °C, respectively. For the hydraulic conductivity, When the COV is 0.05, the SD of the freezing curtain temperature is the smallest. When the COV is 0.15, the SD of the freezing curtain temperature is in the middle. When the COV is 0.25, the SD of the freezing curtain temperature is the largest. The maximum and minimum SD of freezing curtain temperature during the freezing process are 2.56 °C and 0.79 °C, respectively. Different variations of hydrothermal parameters have different effects on the standard deviation of freezing curtain temperature. Different COV parameters have varying impacts on the temperature of the freeze-soft clay rock. The most significant impact comes from thermal

conductivity, followed by permeability coefficient, with specific heat capacity having the smallest effect. Additionally, the larger the COV of the hydrothermal parameters, the greater the SD of the freezing curtain temperature.

Table 4. Parametric influence of different COVs of hydrothermal properties.

Case ID	Thermal Conductivity		Heat Capacity		Hydraulic Conductivity	
	λ_u (W/m/°C)	λ_f (W/m/°C)	C_u(10^6 J/m^3/°C)	C_f (10^6 J/m^3/°C)	K_x^u (10^{-6} m/s)	K_y^u (10^{-6} m/s)
Reference case	0.15	0.15	0.15	0.15	0.15	0.15
COV of thermal conductivity	0.05	0.05	0.15	0.15	0.15	0.15
	0.10	0.10	0.15	0.15	0.15	0.15
	0.15	0.15	0.15	0.15	0.15	0.15
	0.20	0.20	0.15	0.15	0.15	0.15
	0.25	0.25	0.15	0.15	0.15	0.15
COV of heat capacity	0.15	0.15	0.05	0.05	0.15	0.15
	0.15	0.15	0.10	0.10	0.15	0.15
	0.15	0.15	0.15	0.15	0.15	0.15
	0.15	0.15	0.20	0.20	0.15	0.15
	0.15	0.15	0.25	0.25	0.15	0.15
COV of hydraulic conductivity	0.15	0.15	0.15	0.15	0.05	0.05
	0.15	0.15	0.15	0.15	0.10	0.10
	0.15	0.15	0.15	0.15	0.15	0.15
	0.15	0.15	0.15	0.15	0.20	0.20
	0.15	0.15	0.15	0.15	0.25	0.25

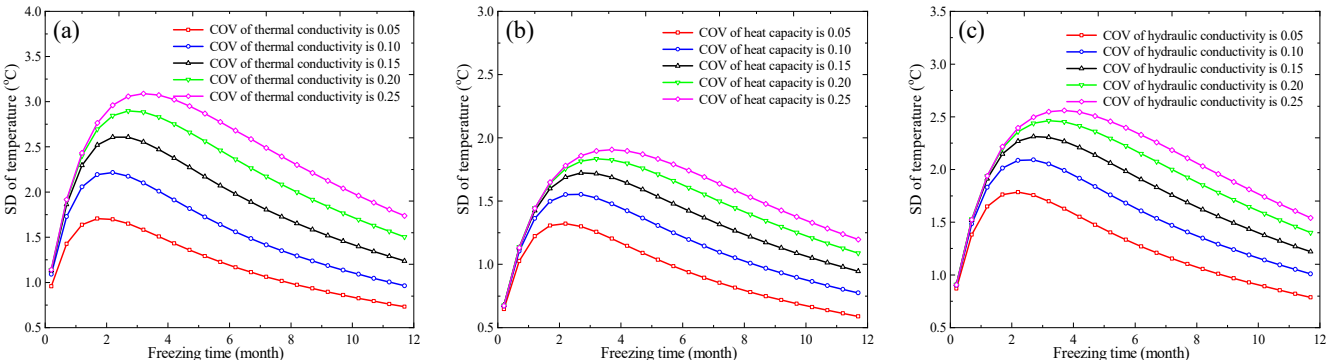

Figure 7. Effects of different COV of variable hydrothermal parameters on uncertain thermodynamic properties: (**a**) Thermal conductivity; (**b**) heat capacity; (**c**) hydraulic conductivity.

4.5. Effect of ACD on Hydrothermal Parameter

Analyzing the autocorrelation distance of thermal parameters in soft clay rock is essential for assessing its impact on freeze curtain temperatures. The autocorrelation distance delineates how thermal properties fluctuate spatially, directly influencing temperature distribution. Understanding this distance aids in optimizing freeze curtain designs to ensure uniform ground freezing and mitigate soil settlement risks during underground space engineering. Incorporating autocorrelation distance into analytical models enhances accuracy, enabling precise predictions of temperature variations along the freeze curtain. This information is vital for informed decision-making in underground space engineering, ensuring the safety, stability, and effectiveness of freeze curtain systems. By considering the autocorrelation distance, engineers can strategically deploy freeze curtain elements, minimizing temperature differentials and promoting reliable ground stabilization. Overall, analyzing the autocorrelation distance of thermal parameters is imperative for comprehen-

sive thermal management in underground space engineering, enhancing project outcomes and safeguarding underground infrastructure. To elucidate the ACD on the temperature characteristics of frozen soft clay rock, this paper selects the 0.4 m, 0.6 m, 0.8 m, 1.0 m, and 1.2 m to represent the ACD of hydrothermal parameters and conducts sensitivity grouping (Table 5) calculations for parameter variability. The results are shown in Figure 8.

Table 5. Parametric influence of different ACDs of hydrothermal properties.

Case ID	Thermal Conductivity		Heat Capacity		Hydraulic Conductivity	
	λ_u (W/m/°C)	λ_f (W/m/°C)	C_u (10^6 J/m^3/°C)	C_f (10^6 J/m^3/°C)	$K_x{}^u$ (10^{-6} m/s)	$K_y{}^u$ (10^{-6} m/s)
Reference case	0.8	0.8	0.8	0.8	0.8	0.8
ACD of thermal conductivity	0.4	0.4	0.8	0.8	0.8	0.8
	0.6	0.6	0.8	0.8	0.8	0.8
	0.8	0.8	0.8	0.8	0.8	0.8
	1.0	1.0	0.8	0.8	0.8	0.8
	1.2	1.2	0.8	0.8	0.8	0.8
ACD of heat capacity	0.8	0.8	0.4	0.4	0.8	0.8
	0.8	0.8	0.6	0.6	0.8	0.8
	0.8	0.8	0.8	0.8	0.8	0.8
	0.8	0.8	1.0	1.0	0.8	0.8
	0.8	0.8	1.2	1.2	0.8	0.8
ACD of hydraulic conductivity	0.8	0.8	0.8	0.8	0.4	0.4
	0.8	0.8	0.8	0.8	0.6	0.6
	0.8	0.8	0.8	0.8	0.8	0.8
	0.8	0.8	0.8	0.8	1.0	1.0
	0.8	0.8	0.8	0.8	1.2	1.2

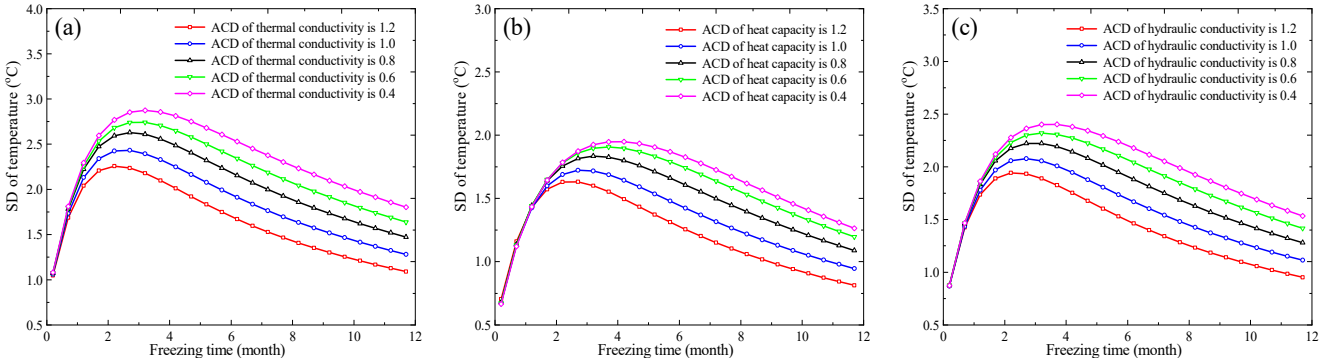

Figure 8. Effects of different ACDs of variable hydrothermal parameters on uncertain thermodynamic properties: (**a**) Thermal conductivity; (**b**) heat capacity; (**c**) hydraulic conductivity.

Figure 8 shows that the five different ACDs have different effects on the SD of freezing curtain temperature. For the thermal conductivity, when the ACD is 0.4 m, the SD of the freezing curtain temperature is the smallest. When the ACD is 0.8 m, the SD of the freezing curtain temperature is in the middle. When the ACD is 1.2 m, the SD of the freezing curtain temperature is the largest. The maximum and minimum SD of freezing curtain temperature during the freezing process are 2.88 °C and 1.05 °C, respectively. For the heat capacity, When the ACD is 0.4 m, the SD of the freezing curtain temperature is the smallest. When the ACD is 0.8 m, the SD of the freezing curtain temperature is in the middle. When the ACD is 1.2 m, the SD of the freezing curtain temperature is the largest. The maximum and minimum SD of freezing curtain temperature during the freezing process are 1.95 °C and 0.67 °C, respectively. For the hydraulic conductivity, When the ACD is 0.4 m, the SD of the

freezing curtain temperature is the smallest. When the ACD is 0.8 m, the SD of the freezing curtain temperature is in the middle. When the ACD is 1.2 m, the SD of the freezing curtain temperature is the largest. The maximum and minimum SD of freezing curtain temperature during the freezing process are 2.40 °C and 0.87 °C, respectively. Different variations of hydrothermal parameters have different effects on the standard deviation of freezing curtain temperatures. Different ACDs of parameters have varying impacts on the temperature of the freeze curtain. The biggest influence is the thermal conductivity, the second is the permeability coefficient, and the least influence is the specific heat capacity. Additionally, the larger the ACD of the hydrothermal parameter, the smaller the SD of the freezing curtain temperature.

5. Conclusions

In this study, the spatial variations of hydrothermal parameters of soft clay rock were calculated based on experimental data. The statistical variability characteristics of variable hydrothermal parameters are estimated. A stochastic coupling model of soft clay rock with heat conduction and porous flow is proposed. According to the relationship between anisotropic spatial variations and statistical variability characteristics for the different random field correlation models, the effects of the ACF, COV, and ACD of variable hydrothermal parameters on underground space engineering are analyzed. The main conclusions obtained are as follows:

(1) The average temperature calculation results of the freezing soft clay rock are close to the experimental results. When the mean temperature approaches 0 °C, there is a noticeable plateau in the curve. The average thickness and temperature of the freezing curtain show an overall increasing trend with increasing freezing time;
(2) From the second month to the tenth month, both the average thickness and temperature increase at a faster rate. When the freezing time reaches twelve months, it tends to stabilize. The overall trend of the SD of the freezing curtain increases with increasing freezing time;
(3) The greater the COV of hydrothermal parameters, the larger the SD of the freezing curtain temperature. For the ACF, the most significant impact comes from DBIN, followed by DSQX, with DSNX having the smallest effect. For COV, the most significant impact comes from thermal conductivity, followed by permeability coefficient, with specific heat capacity having the smallest effect;
(4) Different ACD parameters have varying impacts on the temperature of the freeze-soft clay rock. The biggest influence is the thermal conductivity, the second is the permeability coefficient, and the least influence is the specific heat capacity. The larger the ACD of the hydrothermal parameter, the smaller the SD of freezing soft clay rock temperature.

The variable hydrothermal parameter of soft clay rock holds profound implications for urban underground space sustainable development. As cities continue to expand, the construction and maintenance of underground space infrastructure play a pivotal role in enhancing transportation efficiency, reducing carbon emissions, and fostering economic growth. However, the effectiveness of freeze curtains in controlling water ingress and stabilizing underground space structures depends on the accurate characterization of thermodynamic parameters such as thermal conductivity, permeability coefficient, and specific heat capacity. In the future, we can focus on the dynamic evolution relationship between parameter spatial variability and temperature. By considering the variability in these parameters, urban planners and engineers can make informed decisions that contribute to the sustainability of underground space engineering. Understanding the variable hydrothermal parameters enables the design of freeze curtains that are resilient to changing environmental conditions and geological characteristics. Furthermore, considering variability fosters innovation in sustainable infrastructure development. This aligns with the broader goals of sustainable urban development, which seek to create cities that are livable, equitable, and environmentally conscious. Therefore, the consideration

of variability in thermodynamic parameters of soft clay rock is instrumental in promoting urban sustainable development.

Author Contributions: Formal analysis, T.W.; Investigation, D.W. and H.L.; Resources, J.G.; Data curation, T.W. and K.R.; Project administration, H.L. and J.G.; Funding acquisition, T.W. All authors have read and agreed to the published version of the manuscript.

Funding: This research was supported by the National Natural Science Foundation of China (Grant No. U20B6001, 92255302), the Open Fund of State Key Laboratory of Coal Mining and Clean Utilization (China Coal Research Institute) (Grant No. 2021-CMCU-KF019).

Institutional Review Board Statement: Not applicable.

Informed Consent Statement: Not applicable.

Data Availability Statement: The original contributions presented in the study are included in the article, further inquiries can be directed to the corresponding author.

Acknowledgments: The authors wish to thank three anonymous reviewers and editors for their comments and advice.

Conflicts of Interest: The authors declare no conflicts of interest.

References

1. Long, Y.Y.; Tan, Y. Soil arching due to leaking of tunnel buried in water-rich sand. *Tunn. Undergr. Space Technol.* **2020**, *95*, 103158. [CrossRef]
2. Zhang, S.M.; Li, X.; Li, D.H.; Ding, Z.; Wei, G. Study on failure mode of underground diaphragm wall in soft soil area. *Appl. Mech. Mater.* **2013**, *405*, 1375–1382. [CrossRef]
3. Sousa, R.L.; Einstein, H.H. Lessons from accidents during tunnel construction. *Tunn. Undergr. Space Technol.* **2021**, *113*, 103916. [CrossRef]
4. Ma, E.; Lai, J.; Xu, S.; Shi, X.; Zhang, J.; Zhong, Y. Failure analysis and treatments of a loess tunnel being constructed in ground fissure area. *Eng. Fail. Anal.* **2022**, *134*, 106034. [CrossRef]
5. Liu, J.; Tan, Z.; Zhao, Q.; Liu, B.; Wang, X. Mechanical properties and durability analysis of CS-CG stabilized soil: Towards sustainable subgrade soil enhancement. *Constr. Build. Mater.* **2024**, *442*, 137634. [CrossRef]
6. Ouyang, Z.; Li, P.; Cui, J.; Luo, R.; Yuan, D. Shaking table test study on flexible and rigid immersed tube tunnel in liquefiable soil layer. *Math. Probl. Eng.* **2020**, *2020*, 4980549. [CrossRef]
7. Pimentel, E.; Papakonstantinou, S.; Anagnostou, G.E. Numerical interpretation of temperature distributions from three ground freezing applications in urban tunnelling. *Tunn. Undergr. Space Technol.* **2012**, *28*, 57–69. [CrossRef]
8. Fu, Y.; Hu, J.; Wu, Y. Finite element study on temperature field of subway connection aisle construction via artificial ground freezing method. *Cold Reg. Sci. Technol.* **2021**, *189*, 103327. [CrossRef]
9. Zhao, J.; Yang, P.; Li, L. Investigating influence of metro jet system hydration heat on artificial ground freezing using numerical analysis. *KSCE J. Civ. Eng.* **2021**, *25*, 724–734. [CrossRef]
10. Yue, F.T.; Lv, S.G.; Shi, R.J.; Zhang, Y.; Lu, L. Numerical analysis and spot-survey study of horizontal artificial ground freezing in tunnel connecting passage construction. *Appl. Mech. Mater.* **2015**, *744*, 969–977. [CrossRef]
11. Mauro, A.; Normino, G.; Cavuoto, F.; Marotta, P.; Massarotti, N. Modeling artificial ground freezing for construction of two tunnels of a metro station in Napoli (Italy). *Energies* **2020**, *13*, 1272. [CrossRef]
12. Li, Z.; Chen, J.; Sugimoto, M.; Ge, H. Numerical simulation model of artificial ground freezing for tunneling under seepage flow conditions. *Tunn. Undergr. Space Technol.* **2019**, *92*, 103035. [CrossRef]
13. Liu, X.; Shen, Y.; Zhang, Z.; Liu, Z.; Wang, B.; Tang, T.; Liu, C. Field measurement and numerical investigation of artificial ground freezing for the construction of a subway cross passage under groundwater flow. *Transp. Geotech.* **2022**, *37*, 100869. [CrossRef]
14. Liu, X.; Nowamooz, H.; Shen, Y.; Liu, Y.; Han, Y.; An, Y. Heat transfer analysis in artificial ground freezing for subway cross passage under seepage flow. *Tunn. Undergr. Space Technol.* **2023**, *133*, 104943. [CrossRef]
15. Ma, J.; Huang, K.; Zou, B.; Li, X.; Deng, Y. The influence of tunnel insulation measures on the temperature spatiotemporal variation of frozen soil during artificial ground freezing. *Cold Reg. Sci. Technol.* **2023**, *214*, 103942. [CrossRef]
16. Zhou, J.; Tang, Y. Practical model of deformation prediction in soft clay after artificial ground freezing under subway low-level cyclic loading. *Tunn. Undergr. Space Technol.* **2018**, *76*, 30–42. [CrossRef]
17. Fan, W.; Yang, P. Ground temperature characteristics during artificial freezing around a subway cross passage. *Transp. Geotech.* **2019**, *20*, 100250. [CrossRef]
18. Gao, J.; Li, X.; Cheng, G.; Luo, H.; Zhu, H. Structural evolution and characterization of organic-rich shale from macroscopic to microscopic resolution: The significance of tectonic activity. *Adv. Geo-Energy Res.* **2023**, *10*, 84–90. [CrossRef]
19. Alibeikloo, M.; Khabbaz, H.; Fatahi, B. Random field reliability analysis for time-dependent behaviour of soft soils considering spatial variability of elastic visco-plastic parameters. *Reliab. Eng. Syst. Saf.* **2022**, *219*, 108254. [CrossRef]

20. Elachachi, S.M.; Breysse, D.; Denis, A. The effects of soil spatial variability on the reliability of rigid buried pipes. *Comput. Geotech.* **2012**, *43*, 61–71. [CrossRef]
21. Sun, G.; Peng, F.; Mu, M. Uncertainty assessment and sensitivity analysis of soil moisture based on model parameter errors–results from four regions in China. *J. Hydrol.* **2017**, *555*, 347–360. [CrossRef]
22. Annabi, M.; Raclot, D.; Bahri, H.; Bailly, J.S.; Gomez, C.; Le Bissonnais, Y. Spatial variability of soil aggregate stability at the scale of an agricultural region in Tunisia. *Catena* **2017**, *153*, 157–167. [CrossRef]
23. Wang, F.; Huang, H.; Yin, Z.; Huang, Q. Probabilistic characteristics analysis for the time-dependent deformation of clay soils due to spatial variability. *Eur. J. Environ. Civ. Eng.* **2022**, *26*, 6096–6114. [CrossRef]
24. Kalantari, A.R.; Johari, A.; Zandpour, M.; Kalantari, M. Effect of spatial variability of soil properties and geostatistical conditional simulation on reliability characteristics and critical slip surfaces of soil slopes. *Transp. Geotech.* **2023**, *39*, 100933. [CrossRef]
25. Zhou, Z.; Li, X.; Zhao, H. Probabilistic study of offshore monopile foundations considering soil spatial variability. *ASCE-ASME J. Risk Uncertain. Eng.Syst. Part A Civ. Eng.* **2022**, *8*, 04022035. [CrossRef]
26. Nguyen, T.S.; Likitlersuang, S. Influence of the spatial variability of soil shear strength on deep excavation: A case study of a Bangkok underground MRT station. *Int. J. Geomech.* **2021**, *21*, 04020248. [CrossRef]
27. Wang, T.; Cao, J.; Liu, J.; Xu, J.; Zhou, G. Characterizing anisotropic spatial variations of uncertain mechanical parameters for clay layer using incomplete probability data. *Probabilistic Eng. Mech.* **2024**, *76*, 103623. [CrossRef]
28. Luo, Z.; Hu, B.; Wang, Y.; Di, H. Effect of spatial variability of soft clays on geotechnical design of braced excavations: A case study of Formosa excavation. *Comput. Geotech.* **2018**, *103*, 242–253. [CrossRef]
29. Viviescas, J.C.; Griffiths, D.V.; Osorio, J.P. Geological influence on the spatial variability of soils. *Int. J. Geotech. Eng.* **2022**, *16*, 382–390. [CrossRef]
30. Ching, J.; Uzielli, M.; Phoon, K.K.; Xu, X. Characterization of autocovariance parameters of detrended cone tip resistance from a global CPT database. *J. Geotech. Geoenviron. Eng.* **2023**, *149*, 04023090. [CrossRef]
31. Cai, Y.; Bransby, M.F.; Gaudin, C.; Tian, Y. Accounting for soil spatial variability in plate anchor design. *J. Geotech. Geoenviron. Eng.* **2022**, *148*, 04021178. [CrossRef]
32. Luo, Z.; Di, H.; Kamalzare, M.; Li, Y. Effects of soil spatial variability on structural reliability assessment in excavations. *Undergr. Space* **2020**, *5*, 71–83. [CrossRef]
33. Bong, T.; Stuedlein, A.W. Efficient methodology for probabilistic analysis of consolidation considering spatial variability. *Eng. Geol.* **2018**, *237*, 53–63. [CrossRef]
34. Zhang, W.; Han, L.; Gu, X.; Wang, L.; Chen, F.; Liu, H. Tunneling and deep excavations in spatially variable soil and rock masses: A short review. *Undergr. Space* **2022**, *7*, 380–407. [CrossRef]
35. Cami, B.; Javankhoshdel, S.; Phoon, K.K.; Ching, J. Scale of fluctuation for spatially varying soils: Estimation methods and values. *ASCE-ASME J. Risk Uncertain. Eng.Syst. Part A Civ.Eng.* **2020**, *6*, 03120002. [CrossRef]
36. Yoshida, I.; Tomizawa, Y.; Otake, Y. Estimation of trend and random components of conditional random field using Gaussian process regression. *Comput. Geotech.* **2021**, *136*, 104179. [CrossRef]
37. Gan, X.; Gong, X.; Liu, N.; Yu, J.; Li, W. Random analysis method for nonlinear interaction between shield tunnel and spatially variable soil. *Comput. Geotech.* **2024**, *166*, 105964. [CrossRef]
38. Tounsi, H.; Rouabhi, A.; Jahangir, E. Thermo-hydro-mechanical modeling of artificial ground freezing taking into account the salinity of the saturating fluid. *Comput. Geotech.* **2020**, *119*, 103382. [CrossRef]
39. Sun, Q.; Dias, D. Uncertainty quantification of tunnel seismic deformations in random soils. *Tunn. Undergr. Space Technol.* **2022**, *128*, 104663. [CrossRef]
40. Wang, C.; Wang, K.; Tang, D.; Hu, B.; Kelata, Y. Spatial random fields-based Bayesian method for calibrating geotechnical parameters with ground surface settlements induced by shield tunneling. *Acta Geotech.* **2022**, *17*, 1503–1519. [CrossRef]
41. Cao, J.; Wang, T.; Zhou, G.; Feng, X.; Zhu, C. Parameter estimation of grouting pressure and surface subsidence on the reliability of shield tunnel excavation under incomplete probability information. *Comput. Geotech.* **2024**, *173*, 106530. [CrossRef]